The goal of current research in organic synthesis is to find ways to approach or surpass the finesse shown by nature in the assembly of complex organic molecules. In this work, we have come about as close to achieving this goal as is possible at present. The complete synthesis of the pentacyclic alkaloid **3** requires about ten operations starting with the known, readily available geraniol derivative **5**; the overall chemical yield is 18%. The key transformation, conversion of (*E*)- or (*Z*)-**4** to **3**, utilizes cheap, "low-tech" reagents (potassium hydroxide, ammonia, and acetic acid) and results in the formation of six σ-bonds and five rings (*8*).

REFERENCES AND NOTES

1. S. Yamamura and Y. Hirata, in *The Alkaloids*, R. H. F. Manske, Ed. (Academic Press, New York, 1975), vol. 15, pp. 41–81; ———, *Int. Rev. Sci., Org. Chem. Ser. 2*, **9**, Chap. 6, 161–189 (1976); S. Yamamura, in *The Alkaloids*, A. Brossi, Ed. (Academic Press, New York, 1986), vol. 29, pp. 265–286.
2. R. B. Ruggeri and C. H. Heathcock, *Pure Appl. Chem.* **61**, 289 (1989).
3. E. J. Leopold, *Org. Synth.* **64**, 164 (1985); J. A. Marshall and B. S. DeHoff, *Tetrahedron* **43**, 4849 (1987).
4. S. L. Huang, K. Omura, D. Swern, *J. Org. Chem.* **41**, 3329 (1976); *Synthesis* **1978**, 297 (1978); A. J. Mancuso and D. Swern, *ibid.* **1981**, 165.
5. D. J. Peterson, *J. Org. Chem.* **33**, 780 (1968).
6. K. Bowden, I. M. Heilbron, E. R. H. Jones, B. C. L. Weedon, *J. Chem. Soc.* **1946**, 39 (1946); A. Bowers, T. G. Halsall, E. R. H. Jones, A. J. Lemin, *ibid.* **1953**, 2548 (1953).
7. An azadiene of similar structure has been isolated from a related reaction; see R. B. Ruggeri, M. M. Hansen, C. H. Heathcock, *J. Am. Chem. Soc.* **110**, 8734 (1988).

8. Supported by National Science Foundation grant CHE-84-18437 and by a postdoctoral fellowship granted to S.P. by Merck, Sharp & Dohme Research Laboratories. We thank S. Yamamura for a sample of natural methyl homosecodaphniphyllate and R. Ruggeri, who participated fully in the conception of this biomimetic synthesis [see (*2*)] and discovered a prototype tetracyclization reaction upon which the synthesis is based. Part 6 in a series of papers on the *Daphniphyllum* alkaloids; for part 5, see R. B. Ruggeri, K. F. McClure, C. H. Heathcock, *J. Am. Chem. Soc.* **111**, 1530 (1989).

19 March 1990; accepted 2 May 1990

Regulation of the Timing of Transposable Element Excision During Maize Development

AVRAHAM A. LEVY AND VIRGINIA WALBOT

The ability of transposable elements (TEs) to insert into or excise out of a genetic locus can be regulated by genetic, environmental, and developmental factors. Tissue- or organ-specific activity of TEs is a frequent and well-characterized example of spatial, developmental regulation. Regulation of the timing of TE activity during ontogeny is less well understood. To analyze timing, TE-induced variegation was quantified in the aleurone of maize kernels, a tissue composed of only a single layer of cells, and sector sizes were assigned to specific cell divisions in aleurone development. Three TE families, *Mu*, *Spm*, and *Ac/Ds*, were studied at two genetic loci. It was found that the frequency of transposon excision changes drastically (up to 30-fold increase or equivalent decrease) during the proliferation of the aleurone. Moreover, these changes occur at the same cell divisions in all three TE families. These results suggest that the timing of TE excision during maize development can be controlled by the host.

TRANSPOSABLE GENETIC ELEMENTS (TEs) were first discovered in maize (*1*). Since then, they have been found in all the organisms in which they were sought (*2*). Their ability to generate mutations, by inserting into or excising from a locus, has been exploited for gene analysis and cloning by means of transposon tagging (*3*). In addition, the properties of TEs, such as excision from a reporter gene, have been shown to be under genetic (*1*), environmental (*4*), and developmental (*5, 6*) control. Tissue specificity is the most frequent type of developmental regulation observed with TEs, and the best characterized example of this is the P element of *Drosophila* (*6*). This element is active only in the germ line, not in the soma, as a result of tissue-specific intron splicing (*7*). Similarly, tissue specificity is found for the *Tc* element of *Caenorhabditis elegans* (*8*). In maize, the *Spm* family is more active in the side branches than in the main stalk of the plant (*9*).

A second important aspect of developmental regulation is timing. That is, when during tissue development are TEs most active? Except for the *Mutator* TE family of maize, which has been shown to become germinally (*10*) and somatically (*11*) active late in the development, timing has rarely been investigated, and it is often assumed that TE excision is a stochastic event. One difficulty has been that the cell lineage within a tissue must be known so that TE-induced sectoring can be assigned to specific cell divisions during ontogeny. In this regard, the aleurone of maize is ideal, because the tissue is composed of a single layer of cells whose ontogeny has been elucidated (*12–14*), and this tissue can accumulate anthocyanin pigment. We have monitored the size and appearance of purple sectors produced by excision of three different TE families at two loci in this tissue to calculate the frequency of excision at each cell division of the aleurone. This analysis led to two conclusions: (i) there are changes in excision frequency during development, and (ii) timing appears to be determined by the host rather than by unique properties of the transposable element.

The aleurone is the single-cell epidermal layer of the starchy endosperm of maize kernels and is the site of anthocyanin pigment deposition (*14*). Insertion of a TE in a gene required for anthocyanin synthesis can suppress this purple pigmentation, while excision of the TE can restore it. The size of a revertant sector indicates the number of anticlinal cell divisions that follow the TE excision event, because the presence or absence of this nonvital pigment has no impact on tissue development. We have examined revertant (purple) sectors from three mutable alleles in genetic backgrounds in which somatic instability is maintained. Insertions of *Mu1* (*15*) and *Ds2* (*16*) TEs in the coding region of the *Bz2* locus generated *bz2::mu1* and *bz2::Ds2*, respectively; *c2::Spm* (or *c2-m1*) originated from insertion of an *Spm* TE in the *C2* locus (*17*). *Bz2* and *C2* are loci necessary for the biosynthesis of anthocyanin pigment in most tissues of maize (*18*). Excision of the TEs from these loci can restore gene expression resulting in a purple revertant sector, or spot, on a bronze (*bz2*) or white (*c2*) background in the aleurone.

We have monitored excision events at each stage of aleurone development using video imaging. Developmental stages were defined as the number of divisions at the periphery of the endosperm that contribute to surface growth (anticlinal divisions) and hence to aleurone formation. We defined the stages by the number of cells present using an exponential (powers of two) model of proliferation at the periphery of the endosperm (*12*) (Fig. 1), which allowed assignment of any purple sector to a developmental stage by counting the number of cells in that sector. Our staging system is supported by the model of endosperm development (*12–14*). The maize endosperm is triploid, receiving two haploid nuclei from the maternal parent plus one sperm nucleus. The

Department of Biological Sciences, Stanford University, Stanford, CA 94305–5020.

initial triploid nucleus divides to form a syncytium of synchronously dividing nuclei aligned on the plasma membrane. Subsequently, cellularization occurs, and anticlinal cell divisions at the periphery of the endosperm increase the surface area to form the aleurone, while periclinal divisions fill the internal cavity to form the starchy endosperm. Divisions during the early (syncytial) and late stages of aleurone development are synchronous. Because plant cells do not move relative to each other, the sectors produced by somatic reversion events remain coherent, and the synchronous divisions characteristic of much of aleurone development ensure that cell number is a reliable representation of timing. The development of the starchy endosperm is far more complex than that of the aleurone, because it is derived from both anticlinal and periclinal divisions and is composed of several layers of cells that vary in size and in ploidy level (*14*). Excision events in this tissue, however, do not contribute purple sectors in the aleurone where anthocyanin pigmentation is restricted.

We distinguished two phases in aleurone development that differed radically in the frequency of TE excision events (Fig. 2). In the early stages (divisions 1 to 10), the three mutable alleles differed from each other in excision frequency. The *bz2::mu1* allele showed almost no excision events (Fig. 2A); as noted previously, *Mutator* activities are restricted to late stages in tissue development (*10, 11*). In contrast, the excision frequency ranged from 0.2 to 1.0% for *bz2::Ds2* and *c2::Spm* (Fig. 2, B and C) at these early stages.

In the later stages (after division 10), the three alleles followed the same excision pattern (Fig. 2). Up to division 10, the *bz2::mu1* allele was virtually inactive. Within two to three divisions it became highly active, reaching peak excision rates of 2.4 and 5.6% for one and two doses of the mutable allele, respectively. For the other two alleles, excision rate increased from about 0.6% at division 10 to a maximum of about 1.5% (division 11 to 13). The excision rate decreased during the last four aleurone divisions (divisions 13 to 17), falling to about 0.1% for all three alleles. In the case of *bz2::mu1*, we compared excision frequencies obtained with one or two mutable alleles per cell in order to test for dosage effects. With two doses, excision frequencies

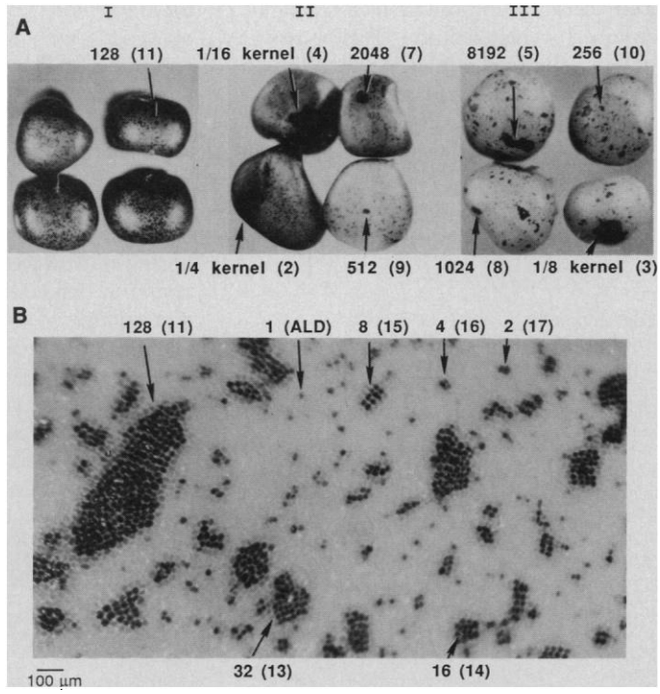

Fig. 1. (**A**) Kernels from stocks used in this study. (I) *bz2::mu1/bz2* (F219) × *bz2/bz2* (F203, *bz2* tester) in which two doses of *bz2::mu1* are present (two lower kernels), and the reciprocal cross in which only one dose of this allele is present (two upper kernels); the origin of these stocks was described previously (*11*); (II) *bz2::Ds2/bz2, Ac* (H218) × *bz2/bz2* (H184, *bz2* tester) has two doses of *bz2::Ds2*; this stock was originally obtained from M. G. Neuffer, and was introgressed into the W23 background; (III) *c2/c2* (ABB105, *c2* tester) × *c2::Spm/c2* (ABB107) has one dose of *c2::Spm*; this stock was originally obtained from E. H. Coe. (**B**) Revertant sectors of intact kernels in the *c2::Spm* stock. Each revertant sector was assigned to a developmental stage; the cell division number is indicated in brackets. This number corresponds to the number of anticlinal divisions. Sectors representing 1/2, 1/4, 1/8, and 1/16 of the whole kernel were scored manually and assigned to an excision event at the first, second, third, and fourth divisions of the endosperm, respectively. Sectors smaller than 1/16 of the kernel were assigned to an anticlinal division at the endosperm surface on the basis of their size: the number of cells in each sector was determined by dividing sector size (in square millimeters) by 0.000625, the average size (in square millimeters) of a single aleurone cell (*11*). Each sector was assigned to a power-of-two-class (2^n) when its number of cells fell in the $2^{n-0.5}$ to $2^{n+0.5}$ range. The *n* value was used as an estimate of the cell division number. Example sectors are indicated by an arrow in (A) and (B). The number of cells (2^n) of the class to which these sectors belong is indicated by the number above the arrows. Sector size was measured at ×50 magnification with a video imaging system equipped with particle analysis software (*11*) (Southern Micro Instruments). Large sectors (divisions 5 to 10) were measured individually from drawings of the contour with the video imaging system. The smaller sectors (divisions 9 to 17) as well as one-cell sectors, which represent an excision event after the last division (ALD, after last division), were counted and measured from scanning across a transect on the kernel's crown (*26*).

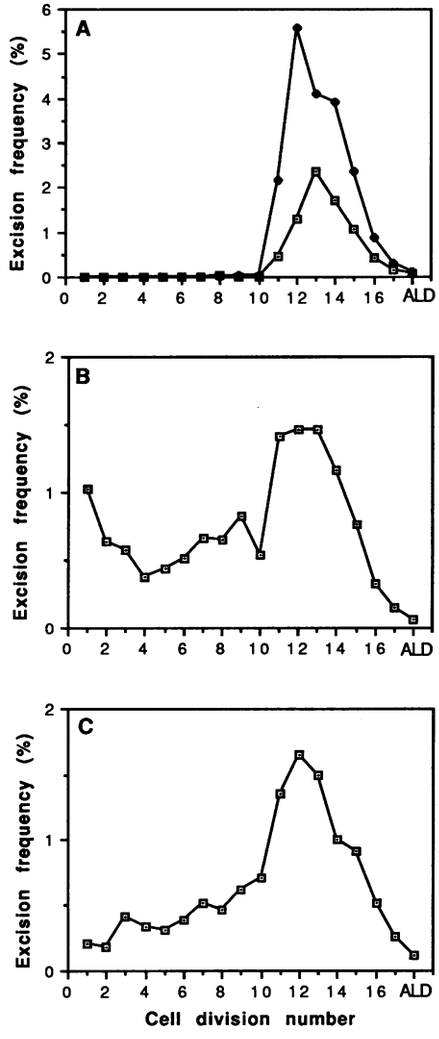

Fig. 2. Variation in excision frequency during aleurone proliferation for three mutable alleles. (**A**) *bz2::mu1* present in one (□) or two (■) doses; (**B**) *bz2::Ds2*; and (**C**) *c2::Spm*. Excision frequency represents the percentage of cells, or nuclei, in which an excision event occurred at a given stage of aleurone proliferation. It was calculated (from data in Table 1) as follows: 100 × (number of excision events scored at a given stage) divided by (number of cells, or nuclei, present in the outer endosperm layer when excision events occurred). The cell division number, or stages of aleurone proliferation, represents the number of anticlinal divisions at the endosperm surface after fertilization (Fig. 1 and Table 1); ALD, after last division. At divisions 9 and 10, excision frequency values were obtained by both measuring individual sectors and by scanning aleurone transects (Table 1). The average of these two values was used here.

doubled at most stages, and there was a shift in the peak of mutability from division 14 to 13. This probably occurred because frequency of excision was so high (up to 5.6%) that some spots from independent events were in contact and hence were interpreted by video imaging as a unique earlier event. This type of sector convergence is not a significant factor with one dose of *bz2::mu1*, because spots covered only 7.5% of the total scanned area. The observation of a linear relation between dosage of the mutable allele and excision frequency observed at each cell division extends earlier studies on other alleles in which only the absolute number of spots of any size (*19*) was compared.

The same pattern of excision frequency, with a maximum around the 13th division, then a 5 to 33% decrease, was observed during aleurone proliferation for mutable alleles containing each of the three different types of TE. The coding capacity of the TE does not seem to be important: *Spm* encodes transposase, whereas *Ds2* and *Mu1* are nonautonomous elements capable of responding to appropriate transposases, but do not encode these functions. The pattern was observed at two loci in the anthocyanin pathway and was independent of the dosage of the mutable allele. Such similarity suggests that TE-encoded regulation of the timing of TE excision during late aleurone development is unlikely, and that the observed regulation is determined by the host.

Several developmental and cellular processes in the endosperm could contribute to the observed excision pattern. First, one or a few periclinal divisions occur from each cell at the periphery of the newly cellularized syncytium to create interior cells, which subsequently proliferate to fill the whole endosperm cavity (*13*). Because only surface sectors were analyzed, such periclinal divisions were not counted. This could result in an underestimate of the number of cell divisions per sector, and hence influence the calculated excision rate at each cell division. The first periclinal division, occurring in each cell of the outer layer of the endosperm, starts after the cellularization stage (divisions 7 to 9) (*13*). Yet, no increase in excision frequency was observed during this period. The last four or five divisions of the aleurone are exclusively anticlinal (*12, 13*). Therefore, periclinal divisions cannot account for the decrease in excision frequency during this period. Second, the length of the cell cycle changes abruptly during endosperm development, from only 8 to 12 hours in the syncytial stage (divisions 1 through 7 require 3 days) to 1 to 3 days after cellularization (divisions 8 through 17 require 3 weeks or more). This decrease in mitotic rate did not correlate with the change in excision frequency. Third, although cellularization is a dramatic event in the developmental history of the endosperm, it does not affect the rate of TE excision. The transition point in excision frequency observed at division 10 is better correlated with the differentiation of the aleurone from the outer endosperm layer starting 10 to 15 days after pollination (*20*).

The underlying molecular mechanisms responsible for the regulation of TE excision remain to be elucidated. Changes in methylation of C residues throughout the genome during aleurone development could indirectly affect the excision of *Mutator* (*21*), *Ac/Ds* (*22*), and *Spm* (*23*) elements. Another possibility is that host factors are required for the excision of TE in higher eukaryotes, as is already established for prokaryotic TE (*24*). The observed excision pattern would then reflect availability of host factors during development. Indeed, the observation that the production of the transposase encoded by the P element of *Drosophila* depends on stage-specific mRNA splicing (*7*) is an example of such a host function.

Whereas *Mutator* seemed previously to be a rare case of timing regulation (*10, 11*), we show here that when TE activity is monitored during development, timing regulation is the rule rather than the exception. Moreover, the timing regulation reported for *Mutator* (*10, 11*) and for the dosage effect of *Ac* (*25*) were examples of element self-regulation, while we show here evidence for host regulation.

The aleurone of maize provides an excellent tissue in which to study timing of TE activity. Control of timing of TE activity in the final divisions of the aleurone is probably of little biological significance for the organism, however, because this tissue is terminally differentiated. On the other hand, host control of the timing of TE activity may affect other cell lineages. For example, in the development of the gametes, alterations in the timing of TE excision would determine the frequency at which mutant and revertant alleles are transmitted to the next generation. In this respect, host regulation of the timing of TE activity may be an interesting example of how development can affect an evolutionary process.

Table 1. Monitoring excision events during aleurone development

Developmental stages	Distribution of revertant sectors obtained with:			
	bz2::mu1 one dose	*bz2::mu1* two doses	*bz2::Ds2*	*c2::Spm*
	*Number of individually scored sectors/number of kernels scored**			
1	0/2000	0/2000	32/1555	4/1000
2	0/2000	0/2000	40/1555	7/1000
3	0/2000	0/2000	72/1555	8/240
4	0/2000	0/2000	21/350	11/200
5	0/2000	0/2000	35/250	12/120
6	0/2000	0/2000	51/150	10/40
7	0/2000	0/2000	39/46	26/40
8	0/2000	0/2000	60/46	24/20
9	10/100	7/100	56/20	31/10
10	9/50	20/50	42/10	35/5
	*Number of sectors scored by scanning kernel surface with video imaging**			
9	0	0	6	3
10	0	5	7	7
11	3	13	29	25
12	17	67	60	61
13	63	99	120	111
14	90	188	191	150
15	114	226	249	272
16	85	167	218	304
17	64	122	193	304
After last division	61	98	155	287

*One transect was scanned on each kernel, and 15 to 40 kernels were used for each stock. A total area corresponding to 84,900, 76,800, 262,400, and 236,800 cells were scanned for *bz2::mu1* one and two doses, *bz2::Ds2*, and *c2::Spm*, respectively.

REFERENCES AND NOTES

1. B. McClintock, *Carnegie Inst. Washington Yearb.* **45**, 176 (1946).
2. D. J. Finnegan, *Trends Genet.* **5**, 103 (1989).
3. C. M. Berg, D. E. Berg, E. A. Groisman, in *Mobile DNA*, D. E. Berg and M. M. Howe, Eds. (American Society for Microbiology, Washington, DC, 1989), pp. 879–925.
4. B. J. Harrison and J. R. Fincham, *Heredity* **19**, 237 (1964); P. J. Kretschmer and S. N. Cohen, *J. Bacteriol.* **139**, 515 (1979).
5. N. V. Fedoroff, *Cell* **56**, 181 (1989).
6. W. R. Engles, *Annu. Rev. Genet.* **17**, 315 (1983).
7. F. A. Laski, D. C. Rio, G. M. Rubin, *Cell* **44**, 7 (1986).
8. J. Collins, B. Saari, P. Anderson, *Nature* **328**, 726 (1987).
9. N. V. Fedoroff and J. A. Banks, *Genetics* **120**, 559 (1988).
10. D. S. Robertson, *Science* **213**, 1515 (1981).

11. A. A. Levy *et al.*, *Dev. Gen.* **10**, 520 (1989).
12. E. H. Coe, Jr., in *Maize Breeding and Genetics*, D. H. Walden, Ed. (Wiley, New York, 1978), pp. 447–459.
13. L. F. Randolph, *J. Agric. Res. (Washington, DC)* **53**, 881 (1936).
14. B. McClintock, *Symp. Soc. Dev. Biol.* **36**, 217 (1978).
15. M. McLaughlin and V. Walbot, *Genetics* **117**, 771 (1987).
16. N. Theres, T. Scheele, P. Starlinger, *Mol. Gen. Genet.* **209**, 193 (1987).
17. U. Wienand, U. Weydemann, U. Niesbach-Kloesgen, P. A. Peterson, H. Saedler, *ibid.* **203**, 202 (1986).
18. E. H. Coe, Jr., and M. G. Neuffer, in *Corn and Corn Improvement*, G. F. Sprague and J. W. Dudley, Eds. (American Society of Agronomy, Madison, WI, 1988), pp. 81–258.
19. M. G. Neuffer, *Genetics* **46**, 625 (1961).
20. D. J. Kyle and E. D. Styles, *Planta* **137**, 185 (1977).
21. V. L. Chandler and V. Walbot, *Proc. Natl. Acad. Sci. U.S.A.* **83**, 1767 (1986).
22. D. Schwartz and E. A. Dennis, *Mol. Gen. Genet.* **205**, 476 (1986).
23. J. A. Banks, P. Masson, N. V. Fedoroff, *Genes Dev.* **2**, 1364 (1988).
24. N. L. Craig and H. A. Nash, *Cell* **39**, 707 (1984).
25. McClintock [B. McClintock, *Cold Spring Harbor Symp. Quant. Biol.* **16**, 13 (1951)] has proposed that increasing dosage of *Ac* causes a delay in the timing of *Ac* action such that transposition occurs only late in the development of the tissue. Schwartz and Echt [D. Schwartz and C. Echt, *Mol. Gen. Genet.* **187**, 410 (1982)], however, have interpreted this dosage effect as being correlated with the physiological state of the cells rather than with the developmental stage of the tissue. In any case, this dosage effect is an example of element-controlled regulation.
26. Although anthocyanin pigment is localized in the vacuole of intact plant cells and should not normally diffuse from cell to cell, lightly colored cells were observed with *bz2::mu1*, *bz2::Ds2*, and *c2::Spm* at the periphery of each spot. The origin of this halo is not known; however, it did not interfere with the sector measurements because the video imaging system was calibrated (object versus background) so that only the dark purple cells were counted as part of a spot.
27. We thank A. Britt for the *c2::Spm* stock and for discussions. Supported by a Chaim Weizmann fellowship (A.A.L.), grants from the National Institute of General Medical Sciences of the NIH (GM 32422) and the USDA (89-37280-4840) to V.W., and an NIH institutional grant to Stanford University for the video imaging equipment.

14 December 1989; accepted 13 April 1990

Binding of Transforming Protein, P47$^{gag\text{-}crk}$, to a Broad Range of Phosphotyrosine-Containing Proteins

MICHIYUKI MATSUDA, BRUCE J. MAYER, YASUHISA FUKUI, HIDESABURO HANAFUSA*

Although the oncogene product of CT10 virus, P47$^{gag\text{-}crk}$, does not itself phosphorylate proteins at tyrosine residues, it elevates phosphotyrosine in transformed cells. The P47$^{gag\text{-}crk}$ oncoprotein contains SH2 and SH3 domains, which are conserved in several proteins involved in signal transduction, including nonreceptor tyrosine kinases. P47$^{gag\text{-}crk}$ bound in vitro to phosphotyrosine-containing proteins from *crk*-transformed cells and from cells transformed by oncogenic tyrosine kinases. The association between P47$^{gag\text{-}crk}$ and p60$^{v\text{-}src}$, a phosphotyrosine-containing protein, was abolished by dephosphorylation of p60$^{v\text{-}src}$. This suggests that the SH2 and SH3 regions function to regulate protein interactions in a phosphotyrosine-dependent manner.

MANY PROTEINS INVOLVED IN SIGnal transduction contain common domains, named SH2 and SH3 (*src* homology 2 and 3), which were originally found in the regulatory regions of nonreceptor tyrosine kinases (*1–3*). Although regulatory functions for these domains were suggested from mutational analyses, their biological function is still unclear (*4*). Because P47$^{gag\text{-}crk}$ consists almost entirely of SH2 and SH3 domains (*5*), which are indispensable for transformation by this oncogene product (*6*), analysis of transformation by P47$^{gag\text{-}crk}$ should provide an understanding of the function of the SH2 and SH3 regions.

Several cellular phosphoproteins from CT10-transformed cells coimmunoprecipitate with P47$^{gag\text{-}crk}$ and antibodies to Gag (anti-Gag) or Crk (anti-Crk) (*7*). These cellular phosphoproteins are identical, as judged by V8 protease mapping, to those precipitated from lysates of the same cells, with an antibody to phosphotyrosine (anti-phosphotyr) (*7*). These results suggest that the proteins phosphorylated on tyrosine are bound to P47$^{gag\text{-}crk}$.

To examine the specificity of the interaction among these proteins, we performed immunoprecipitations in the presence of an excess of exogenously added P47$^{gag\text{-}crk}$. ^{32}P-labeled cellular proteins of 135, 120, 94, 87, and 65 to 75 kD were precipitated from lysates of *crk*-transformed 3Y1 cells (Crk-3Y1) (*8*) by anti-phosphotyr (Fig. 1, lane 4). P47$^{gag\text{-}crk}$ that was immunoprecipitated with antibody to p19^{gag} (anti-p19^{gag}) was associated with nearly all of the phosphotyrosine-containing proteins (Fig. 1, lane 3). The only protein detectable by anti-phosphotyr but not coimmunoprecipitated with anti-p19^{gag} was the 120-kD protein (Fig. 1, lane 5). The 120-kD protein was probably difficult to detect by immunoprecipitation with anti-p19^{gag} because it was weakly associated with P47$^{gag\text{-}crk}$. Therefore, we used beads coupled to recombinant P47$^{gag\text{-}crk}$ by means of anti-p19^{gag} (P47$^{gag\text{-}crk}$–anti-p19^{gag} complex) (*9*) to coimmunoprecipitate the 120-kD protein from the fraction of the lysate not bound by anti-p19^{gag} alone (Fig. 1, lane 6). If the cell lysate was first treated with anti-phosphotyr, no phosphoproteins were detected in supernatant subjected to immunoprecipitation by anti-p19^{gag} or the P47$^{gag\text{-}crk}$–anti-p19^{gag} complex (Fig. 1, lanes 7 and 8). These results suggest that P47$^{gag\text{-}crk}$ associates with phosphoproteins that contain phosphotyrosine and with few, if any, phosphoproteins that contain only phosphoserine or phosphothreonine.

To see whether P47$^{gag\text{-}crk}$ bound a broad spectrum of phosphotyrosine-containing proteins, we examined the binding of purified P47$^{gag\text{-}crk}$ in vitro to proteins phos-

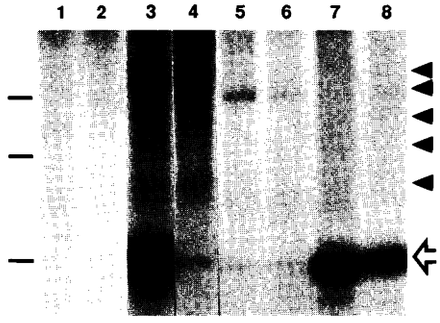

Fig. 1. Association of phosphotyrosine-containing proteins with P47$^{gag\text{-}crk}$ (*18*). [^{32}P]Orthophosphate-labeled proteins from 3Y1 (lanes 1 and 2) and *crk*-transformed 3Y1 (Crk-3Y1) cells (lanes 3 to 8) were precipitated with anti-p19^{gag} (3C2 monoclonal antibody (*19*) (lanes 1 and 3) or anti-phosphotyr (*20*) (lanes 2 and 4). Protein (50 μg) from Crk-3Y1, which contained ~0.01 μg of P47$^{gag\text{-}crk}$, was used in each lane. Supernatants from these immunoprecipitations were immunoprecipitated with a second set of antibodies: supernatant of anti-p19^{gag} immunoprecipitation (lane 3) was precipitated with anti-phosphotyr (lane 5) or with anti-p19^{gag} coupled with 0.5 μg of recombinant P47$^{gag\text{-}crk}$ produced in insect cells (P47$^{gag\text{-}crk}$–anti-p19^{gag} complex) (*9*) (lane 6); supernatant of anti-phosphotyr immunoprecipitation (lane 4) was precipitated with anti-p19^{gag} (lane 7) or the P47$^{gag\text{-}crk}$–anti-p19^{gag} complex (lane 8). Immunoprecipitates were analyzed by SDS–polyacrylamide gel electrophoresis (SDS-PAGE) (10% gel). Arrowheads indicate the major phosphotyrosine-containing proteins in Crk-3Y1 cells (from top of gel): 135, 120, 94, 87, and 65 to 75 kD. P47$^{gag\text{-}crk}$ is indicated by the open arrow. Bars at the left of the figure are molecular size markers: 110, 84, and 47 kD.

The Rockefeller University, New York, NY 10021.

*To whom correspondence should be addressed.